Published in final edited form as:
Glia. 2009 August 1; 57(10): 1115–1129. doi:10.1002/glia.20835.

Developmental and Post-Injury Cortical Gliogenesis: A Genetic Fate-Mapping Study with Nestin-CreER Mice

Kevin A. Burns[1], **Brian Murphy**[2,3], **Steve C. Danzer**[2], and **Chia-Yi Kuan**[1,4]

[1]Divisions of Developmental Biology and Neurology, Cincinnati Children's Hospital Medical Center, Cincinnati, OH 45229

[2]Departments of Anesthesia and Pediatrics, Cincinnati Children's Hospital Medical Center, Cincinnati, OH 45229

[3]Program in Neuroscience, University of Cincinnati, Cincinnati, OH 45229

Abstract

The primary sources of cortical gliogenesis, either during development or after adult brain injury, remain uncertain. We previously generated Nestin-CreER mice to fate-map the progeny of radial glial cells (RG), a source of astrocytes and oligodendrocytes in the nervous system. Here, we show that Nestin-CreER mice label another population of glial progenitors, namely the perinatal subventricular zone (SVZ) glioblasts, if they are crossed with stop-floxed EGFP mice and receive tamoxifen in late embryogenesis (E16-E18). Quantification showed E18 tamoxifen-induction labeled more perinatal SVZ glioblasts than RG and transitional RG combined in the newborn brain (54% vs. 22%). Time-lapse microscopy showed SVZ-glioblasts underwent complex metamorphosis and often-reciprocal transformation into transitional RG. Surprisingly, the E10-dosed RG progenitors produced astrocytes, but no oligodendrocytes, whereas E18-induction fate-mapped both astrocytes and NG2+ oligodendrocyte precursors in the postnatal brain. These results suggest that cortical oligodendrocytes mostly derive from perinatal SVZ glioblast progenitors. Further, by combining genetic fate-mapping and BrdU-labeling, we showed that cortical astrocytes cease proliferation soon after birth (<P10) and only undergo non-proliferative gliosis (i.e. increased GFAP expression without cell-division) after stab-wound injury in adult brains. By contrast, 9.7% of cortical NG2+ progenitors remained mitotic at P29, and the ratio rose to 13.8% after stab-wound injury. Together, these results suggest NG2+ progenitors, rather than GFAP+ astrocytes, are the primary source of proliferative gliosis after adult brain injury.

Keywords

Subventricular zone (SVZ)-glioblasts; Radial Glia (RG); Gliogenesis; Gliosis; Oligodendrocyte; Astrocyte

Correspondence to: Chia-Yi Kuan.

Correspondence should be address to: Chia-Yi Kuan, MD, PhD (alex.kuan@cchmc.org) Division of Developmental Biology and Neurology Cincinnati Children's Hospital Medical Center S3.421, 3333 Burnet Avenue, Cincinnati, OH 45229. [4]Corresponding author.

INTRODUCTION

The lineage origins of cortical macroglia (astrocytes and oligodendrocytes) and their proliferative potential following adult brain injury remain uncertain (Goldman, 2001; Kessaris et al, 2006). Radial glial cells (RG), besides producing neurons and supporting neuronal migration during embryogenesis (Noctor et al., 2001; Rakic, 2003), are often considered a principle source of cortical macroglia because of their morphological transformation into astrocytes (Schemechel and Rakic, 1979; Voigt, 1989; Culican et al., 1990). This view is also supported by the finding of radial precursors of both astrocytes and oligodendrocytes in the spinal cord (Hirano and Goldman, 1988). However, a recent study using GLAST-CreER mice to fate-map the progeny of RG progenitors only detected few oligodendrocytes in the postnatal cerebral cortex (Mori et al., 2006). This result implicated non-RG oligodendrocyte progenitors in the forebrain.

Another important source of cortical macroglia is the perinatal subventricular zone (SVZ) glioblasts, which, unlike RG, do not project long processes to the pial surface (Goldman, 2001). The existence of glioblasts in the perinatal SVZ was originally suggested by thymidine labeling experiments, and more recently shown by injection of replication-incompetent retrovirus into the newborn brain (Fujita, 1965; Levison and Goldman, 1993). Time-lapse videomicroscopy showed that perinatal SVZ glioblasts can migrate to the cortex and generate both astrocytes and oligodendrocytes after several rounds of cell-division (Kakita and Goldman, 1999). However, because retroviral infection labels only a few cells at a time, the relative contributions by RG and perinatal SVZ glioblasts to cortical gliogenesis are unknown.

Another unresolved issue in cortical gliogenesis is whether mature astrocytes can proliferate after injury in adult brains. The traditional view holds that stab wound to adult brains only induces astrocytes to synthesize more glial-fibrillary acidic protein (GFAP) without proliferation, whereas NG2+ progenitors can divide and generate new oligodendrocytes and astrocytes after injury (Levine et al., 2001; Alonso, 2005; Baracskay et al., 2007). Yet, a recent genetic fate-mapping study using GLAST-CreER mice concluded that GFAP+ astrocytes are the principle source of glial proliferation after stab-wound injury to adult brains (Buffo et al., 2008). This unexpected finding warrants further investigation.

We previously generated Nestin-CreER mice, which when crossed to stop-floxed enhanced green fluorescence protein (EGFP) reporter mice and following tamoxifen-induction, can label RG progenitors and their progeny (Burns et al., 2007). Here, we show that Nestin-CreER mice can also label perinatal SVZ-glioblasts after tamoxifen induction in late embryogenesis. This property allows comparison of the contributions by RG and perinatal SVZ glioblasts to cortical gliogenesis. Furthermore, we used the combination of genetic fate-mapping and BrdU immunocytochemistry to examine the source of post-injury glial proliferation. Our results indicate that NG2+ progenitors, rather than GFAP+ astrocytes, are the primary source of post-injury cortical gliogenesis.

MATERIALS AND METHODS

Tamoxifen dosing

Tamoxifen (Tam) (Sigma, St. Louis, MO) was dissolved at 10-20mg/mL in corn oil. Bi-transgenic Nestin-CreER/EGFP-Cre-Reporter pregnant dams were injected intra-peritoneally with 1 to 2 mg Tam on the indicated embryonic days. Detection of the vaginal plug was considered E0.5.

Histology

Animals were sacrificed by overdose of 2.5% Avertin (1:1 w/v 2,2,2-Tribromoethanol Acros Geel, Belgium/t-amyl alcohol, Sigma) in 0.9M phosphate buffered saline (PBS) followed by transcardial perfusion of ice cold PBS, and 4% paraformaldahyde (Acros) in PBS. Brains were post-fixed in 4% paraformaldehyde overnight at 4°C and dehydrated in 30% sucrose at 4°C over two days. They were then immersed in Optimal Cutting Temperature medium (Sakura Finetek, Torrance, CA) for 30 minutes and flash frozen in isopentane [2-methylbutane (Sigma)] chilled with dry ice. 30-50 micron-thick sections were cut using a Leica cryostat. Antibodies were diluted in 1% bovine serum albumin (Fischer Scientific, Fair Lawn, NJ) and 0.1% Triton X-100, in PBS. Antibodies used were EGFP (1:500 Mouse, Molecular Probes, Eugene, OR), EGFP (1:1000 Rabbit, Molecular Probes), GFAP (1:1000 Mouse, Chemicon, Temecula, CA), GFAP (1:500 Rabbit, Dako, Fort Collins, CO), NG2 (1:400 Rabbit, Chemicon), RIP (1:1000 Mouse, Chemicon), BrdU (1:500 Rat, Serotec, Raleigh, NC), Nestin (1:1000 Mouse, Chemicon), Olig2 (1:1000 Rabbit, Chemicon).

Organotypic Slice Cultures and Time-Lapse Microscopy

Bi-transgenic animals were induced with tamoxifen on either E16 or E18. Animals were then sacrificed by cervical dislocation (dams) or decapitation (embryo or newborn) on E17, E18, or P0 leaving at least one day between tamoxifen induction and sacrifice to allow time for EGFP to be expressed. . The brain was then mounted on a tissue slice chuck (Campden Instruments, Lafayette, IN), and 400μm coronal slices of cortex were cut using the MA752 motorized advanced vibra-slice (Campden Instruments) while bathed in ice-cold dissection buffer [Gey's Balanced Salt Solution (Sigma-Aldrich, St. Louis, MO) plus 6.5mg/ml glucose (Sigma-Aldrich), pH 7.2]. Explants were cultured using the interface method (Stoppini et al., 1991). Briefly, two to three slices were plated onto Millicell inserts (Millipore, Bedford, MA) in 35 mm sterile Petri dishes (Fisher Scientific) with 1.1 ml of Stoppini medium media [50% minimal essential medium, 25% hanks buffered salt solution, 25% heat inactivated horse serum, 10mM HEPES, 0.5% GlutaMax (all from Invitrogen, Carlsbad, CA) and Glucose (0.65g/100ml; Sigma-Aldrich)] and incubated at 37°C in a 5% CO_2/95% air mix at 100% humidity for three hours before live-imaging. Brain slices were imaged every hour using a Leica SP5 confocal microscope equipped with 10X (0.3 NA) objective. Z-stack image series were collected at 5-7μm increments through the depth of the tissue. Explants were encased in a culture chamber and continually perfused with 5% CO_2/95% air mix at 100% humidity. The chamber was kept at 37°C in a Luden chamber during imaging. Culture media was changed every two days.

Postnatal proliferation and needlestick injury model

Animals were dosed with tamoxifen on E18.5. For the postnatal glia proliferation study, 3 groups (n=3 each) were dosed with 100mg/kg body weight of 5-Bromo-2′-deoxyuridine (BrdU) (Sigma) once a day for three days during the following intervals P2-P4, P10-P12, or P27-P29. Animals were sacrificed on P31. For the needlestick injury model, bi-transgenic animals were again induced with tamoxifen on E18.5. Starting on P42, animals (n=4) were dosed with BrdU once a day for seven days. On the fourth day of dosing, animals were anesthetized with isoflurane and, using a stereotaxic apparatus, subjected to two needlestick wounds 2 mm deep on the right side of the brain at Bregma +.9 mm and Bregma -1.7 mm using a 25G syringe needle. Animals were sacrificed the day after the final dose of BrdU.

Imaging and Cell Counting

Samples were visualized using either an Olympus epifluorescent microscope (BX-51) (low power images only) or a Zeiss confocal microscope (LSM-510). For cell counting, a 10x image of the cortex was captured. Individual cells in the same field were then examined by eye at high power (20-40x) to determine their cell type, which was then marked over the cell in Adobe Photoshop using color-coded icons, which were later independently tabulated. Cells were counted only if they were above the intermediate zone or sub-cortical white matter. BrdU co-localization was determined by toggling between red and green filters and scrolling through the z-plane of each cells nucleus and later confirmed by confocal microscopy. In the needle-stick injury model, only EGFP+ cells within 1.5mm on either side of the wound were tabulated. This region included areas without increased GFAP expression.

Statistical analysis

Comparisons in proliferation were performed with a paired two-tailed student's t-test using Microsoft excel.

RESULTS

Nestin-CreER mice label cortical radial glial and subventricular zone progenitors

We previously generated mice using the Nestin second intron enhancer (NIE) to express a tamoxifen-inducible form of Cre recombinase (CreER) (Burns et al., 2007). We have shown that Nestin-CreER mice, when crossed with a stop-floxed EGFP reporter line and prenatally dosed with tamoxifen can be used to fate-map the progeny of embryonic neuroglial progenitors.

To further characterize the embryonic progenitors labeled with this system, we injected one dose of tamoxifen (1-2 mg) to pregnant mice at embryonic (E) 10.5 day, and collected the animals at E12.5 for analysis. This induction-chase protocol (E10Tam-E12) labeled numerous cells in the midbrain and the ventral telencephalon, but few in the E12.5 cerebral cortex (Fig. 1A, B), consistent with the relatively late onset of cortical neurogenesis during embryogenesis. The EGFP+ cells in the cerebral cortex displayed a variety of morphologies (Fig. 1E-H), including RG with a long vertical process extended to the pia, “short neural precursors” possessing a ventricular end-foot and a basal process of variable length (asterisk

in Fig. 1E, G; Gal et al., 2006), and putative Cajal-Retzius (CR) cells underneath the pial surface (Fig. 1G). Double-labeling showed most EGFP+ cells near the ventricular surface co-expressed Nestin (Fig. 1F-H). Conversely, the EGFP+ cells distant from the ventricular zone were negative for anti-Nestin staining, suggesting they were the progeny of Nestin+ progenitors. The EGFP-labeling was tamoxifen dependent because, without tamoxifen induction, no EGFP+ cell was found in Nestin-CreER: stop-floxed EGFP embryos (hereafter referred to as bitransgenic embryos) (Fig. 1C, D).

When tamoxifen was injected at E18.5 and pups collected at postnatal day 1 (P1), many cells were labeled in the subventricular zone (SVZ) of the newborn cerebral cortex (Fig. 1I-L). These included few RG (arrows in Fig. 1J, K) and many glial cells with a relatively simple morphology, when compared to those in mature brains (described in Figure 3). Together, these results suggest that Nestin-CreER embryos can be used to label cortical RG or SVZ progenitors depending on the timing of tamoxifen induction.

Genetic fate-mapping in the cerebral cortex

To compare cell types derived from NIE-positive precursors of different stages of cortical histogenesis, we administered tamoxifen to bi-transgenic embryos at E10.5 (early-), 14.5 (mid-), or 18.5 (late cortical histogenesis), and examined the distribution and identity of EGFP+ cells in the P30 forebrain.

This analysis showed that E10.5-tamoxifen injection labeled pyramidal neurons in all cortical layers (Fig. 2A, D). E14.5-induction labeled those in upper cortical layers following the inside-out sequence of cortical neurogenesis (Fig. 2B, E). But no cortical pyramidal neurons were labeled by E18.5-dosing (Fig. 2C, F), despite this induction protocol labeled many dentate gyrus granule cells, the CA pyramidal neurons (Fig. 2J) and olfactory interneurons (data not shown), consistent with their respectively perinatal and postnatal birthdates.

In addition, each tamoxifen-induction scheme labeled astrocytes (asterisks in Fig. 2A-F). In contrast, only E14.5- and E18.5-dosing, but not E10.5-tamoxifen induction labeled oligodendrocytes in the postnatal cerebral cortex (Ctx) and the corpus callosum (CC) (Fig. 2G-I). Table 1 summarizes the progeny cell-types of Nestin+ precursors after tamoxifen induction at varying time-points. Together, these results indicate early divergence of cortical astrocyte and oligodendrocyte lineages during embryogenesis.

Static and live-imaging analysis of perinatal cortical gliogenesis

Because E18.5-tamoxifen induction exclusively labeled astrocytes and oligodendrocytes in the postnatal cerebral cortex (Fig. 2C), this induction scheme provides a unique tool to study cortical gliogenesis. Thus, we used both histological methods and time-lapse microscopy to examine the morphological maturation of cortical macroglia.

Static imaging in the cerebral cortex of E18 tamoxifen-induced animal revealed EGFP+ cells with simple morphology and little branching from birth through P2 (Fig. 3A, a). By P4, a greater number of EGFP+ cells possessed more elaborated branching (Fig. 3B, b). At P7, EGFP+ cells in the cortex appeared fairly mature and displaying a complex branching

pattern (Fig. 3C, c). Moreover, the number of EGFP+ cells in the subventricular zone increased from birth to P4, and decreased after P7 (rectangles in Fig. 3A-C and the enlarged images in Fig. 3a′-c′).

We also used slice preparation and time-lapse video microscopy to examine the behavior of EGFP+ RG and SVZ glioblasts in the perinatal brain, for comparison with those described following retroviral infection (Kakita and Goldman, 1999). To ensure sufficient EGFP expression for live imaging, we induced bitransgenic embryos with tamoxifen at E16, and began slice cultures on E18. Although E16-induction labeled a few ventral telencephalon-derived interneurons, their tangential migration in the marginal zone makes them easily distinguishable from those of RG and the SVZ glioblasts.

At the beginning of time-lapse imaging, we found that the majority of EGFP+ cells showed a simple bipolar morphology in the cortical plate as well as the SVZ/VZ of E18 brain slices. Over the course of a four-day culture, EGFP+ cells in the SVZ/VZ migrated actively into the cortical plate and underwent extensive bifurcation of the cytoplasmic processes (n=6; Fig. 3D, also see Supplementary Movie 1). Together, these results indicate that the slice preparation recapitulates many salient features of in-vivo cortical gliogenesis.

Migration and cell-division of perinatal SVZ glioablasts

Live-imaging analysis also revealed two distinct patterns of glioblats migration: the translocation mode and the locomotion mode (Fig. 4A, B). In the translocation mode, EGFP + SVZ/VZ cells ascend through the whole-depth of intermediate zone (IZ) by nuclear and somal translocation along a long leading process towards the pial surface, accompanied by retraction of the trailing process (Fig. 4A, see Supplementary Movie 2). In the locomotion mode, EGFP+ cells with a short leading process leave the SVZ soon after their appearance, and migrate through the overlaying presumptive white matter into the cortical plate (Fig. 4B, see Supplementary Movie 3). We found the locomotion mode to be the predominant pattern of migration for SVZ glioblasts, consistent with a previous study using retrovirus to label SVZ glioblasts (Kakita and Goldman, 1999).

Further, live-imaging revealed that SVZ glioblasts actively proliferate within the cortical plate. Glioblasts often adopt a symmetric mode of cell-division, with each of two daughter cells undergoing a subsequent round of mitosis over a period of 24 hrs (Fig. 4C, see Supplementary Movie 4).

Together, these live-imaging experiments revealed many common features of SVZ glioblasts detected by either the Nestin-CreER system or the retroviral infection method (Levison and Goldman, 1993; Kakita and Goldman, 1999).

Classification and quantification of glial cell-types during cortical gliogenesis

Next, we compared the percentage of labeled glioblasts and maturing macroglia in the cortex from birth to P10. Since the EGFP-reporter mice used in our study show detailed cellular morphology, we were able to distinguish six classes of EGFP+ cells. In selected sections, we also performed double-labeling to verify the identity of morphologically

defined glioblasts and cells (Fig. 5, see also Supplementary Figure 1). The EGFP+ classes are:

1. Radial glia: these cells have a simple ovoid cell body and a long vertical fiber stretching across the cortex with end-feet on the pial surface or blood vessels (Fig. 5A). These long vertical fibers were often positively stained for two well-characterized RG-markers: Nestin (Fig. 5G; Malatesta et al., 2000) and the glutamate transporter (GLAST).
2. Transitional/Bipolar cells: these cells possess a vertical process that is shorter but thicker than RG fibers, and multiple non-radial processes sprouting from the fiber shaft or cell body (Fig. 5B). These features are similar to those previously described for transforming RG (Schmechel and Rakic, 1979; Takahashi et al., 1990).
3. Simple glioblasts: these cells contain an oval-shaped cell body and short, simple cytoplasmic processes (Fig. 5C). They are positioned in the dorsolateral SVZ, but also exist in the cortex proper (Fig. 4B). Double-labeling showed simple glioblasts often express Nestin (Fig. 5H) and Olig2 (Fig. 5I), a marker of glial progenitors in the postnatal brain (Marshall et al., 2005; Cai et al., 2007).
4. Polydendritic glioblasts: the processes of these cells are of comparable length and spherical arrangement of processes to those of mature astroglia, but lack high order secondary branching (Fig. 5D). Double-labeling showed these polydendritic cells also express Olig2 (Fig. 5J) and often incorporate BrdU given shortly before sacrifice (Fig. 6F). Thus, they were classified as “glioblasts”.
5. Mature astrocytes: these cells have a dense veil of highly bifurcated processes (Fig. 5E). Not all mature astrocytes express GFAP, and if they do, the GFAP expression is restricted to proximal portions of the processes (Fig. 5K).
6. Oligodendrocytes: these cells exhibit lacy processes arranged as parallel sheets in the white matter (Fig. 2H, I) or as spherical protrusions in the grey matter (Fig. 5F), which are distinct from those of mature astrocytes. Furthermore, these cells express RIP (Fig. 5L), which specifically recognizes the 2′, 3′-cyclic nucleotide 3′-phosphodiesterase in oligodendrocytes (Watanabe et al., 2006).

Using the above morphological criteria, we quantified EGFP+ cells in the perinatal brain of bitransgenic animals following tamoxifen-induction at E18.5. After birth, the percentage of RG and transitional forms declined from 35% at P2 (43/121; Table 2) to less than 2% at P10 (6/375). Simple and polydendritic glioblasts are the predominant cell type through P4 (72.5%, 415/572), but are gradually replaced by mature astrocytes and oligodendrocytes, which together reach 72% of all labeled cells by P10 (272/375). However, even at P10, simple glioblasts constituted 13.3% (50/375) and polydendritic glioblasts represented 26.4% (99/375) of all EGFP+ cells.

Morphological transformation of glial cell types revealed by live imaging

Live-imaging also revealed complex and often-reciprocal metamorphosis between various forms of glioblasts (Fig. 6A, see Supplementary Movie 5). For example, simple glioblasts

could unilaterally extend a singular cytoplasmic process, thus resembling transitional RG (Fig. 6B). Also, bipolar transitional cells could undergo mitosis to produce two simple glioblasts (Fig. 6C) or two polydendritic glioblasts (Fig. 6D). Simple glioblasts could directly transform into polydendritic glioblasts (Fig. 6E,). Live imaging and BrdU-immunocytochemistry also indicate polydendritic glioblasts can undergo mitosis without retracting their long processes (Fig. 6F).

Together, the live-imaging results highlight a high degree of morphological flexibility amongst glioblasts as previously suggested (Hunter and Hatten, 1995), which cautions against the strict interpretation of “transitional forms” as direct descendants of RG.

The time-frame of cortical gliogenesis in postnatal brains

For a study of post-injury gliosis in adult brains, we needed to establish the baseline temporal window for cortical gliogenesis in bitransgenic animals. To do so, we labeled cortical macroglia via E18-tamoxifen induction and injected one dose of BrdU (100μg/g of body weight) per day to the resultant bitransgenic mice for three consecutive days starting at P2, P10, or P27. All animals were sacrificed at P31, and the brains were processed anti-BrdU/EGFP immunostaining. This analysis indicated the number of BrdU-labeled cells markedly declined in the first postnatal month (Fig. 7A-C), in accord with the results in previous studies (reviewed in Sauvageot and Stiles, 2002).

Next, we compared the ratio of BrdU-incorporated, EGFP-expressing astrocytes and oligodendrocytes in the first postnatal month, as an index of their proliferative capacity. We found that the percentage of BrdU-labeled EGFP+ astrocytes fell quickly from 33.1% at P2-P4 (60/181, n=3) to 2.5% at P10-12 (5/181, n=2), and none by P27-P29 (0/220, n=3) (Fig. 7D-F, M). In contrast, EGFP+ oligodendrocytes were labeled by BrdU throughout the first postnatal month, including 50.7% labeled with P2-4 BrdU dosing (43/88, n=3), 16.3% labeled with P10-12 dosing (12/73, n=2), and 9.7% labeled by P27-29-dosing (15/156, n=3).

Moreover, BrdU-labeled oligodendrocytes most often appeared as doublets (Fig. 7G-I), especially in mice dosed with BrdU after P10. The distinct morphology of these cells (e.g. lacking complex branching as astrocytes and parallel processes of myelinating oligodendrocytes) is similar to that of immature oligodendrocyte precursors (OPCs) described in previous studies (Levine et al., 2001). Moreover, double-labeling showed that almost all EGFP+ cells with this morphology express NG2 proteoglycan (Fig. 7J-L), a well-established marker for OPCs (Baracskay et al., 2007). Together, these results reveal a short period of cortical astrocyte production (< P10), in contrast to prolonged proliferation by NG2+ OPC in the postnatal brain.

Nature of reactive gliosis following a stab wound to adult brains

Next, we combined genetic fate-mapping and BrdU immunocytochemistry to examine the nature of “reactive gliosis” after adult brain injury. To do so, bitransgenic animals were induced with tamoxifen at E18, subjected to a needle-stick stab-wound on P45, and sacrificed on P49. These mice also received daily BrdU injection from P42 to P48 (i.e. spanning from three days before to three days after the insult). The gliosis response was

evaluated by the percentage of GFAP+ cells among EGFP+ astrocytes (Fig. 8), and the ratio of BrdU-labeled cells among EGFP+ astrocytes and OPCs (Fig. 9).

We found that the stab-wound injury caused a clear increase of GFAP-expressing astrocytes along the track of needle-stick insertion (Fig. 8A). Double-labeling indicated there was also an increase of EGFP+ astrocytes and OPCs near the needle-stick track (Fig. 8B). Likewise, the number of EGFP/GFAP double-positive cells greatly increased near the lesion site (29.3%, 388 cells counted, Fig. 8D, E) compared to the contralateral side (2.4%, 357 cells counted, Fig. 8E) (n=4). Moreover, the GFAP expression extended from the proximal portion to distal branches of EGFP+ astrocytes on the lesioned side (arrows in Fig. 8D). Together, these results indicate that a significant gliosis response was induced.

However, when the percentages of BrdU-labeled, EGFP+ astrocytes on the stab-wound injured side were compared to the contralateral side, we found no evidence of increased proliferation amongst fate-mapped astrocytes (Fig. 9A-C, G; both at 1.1-1.3%, 239 cells counted; n=4). In contrast, there was a trend of incresing BrdU-incorporation among OPCs (compare Fig. 9D to 7J) in the injured cortex (13.8%, 191 cells counted), when compared to 9.1% (17/183 cells) on the contralateral side (Fig. 9D-F, H; p=0.16 by two-tailed student's *t*-test, n=4).

Together, these results suggest the gliosis response by astrocytes follwoing stab-wound injury is primarily non-proliferative hypertrophy, while OPCs possess a greater potential for post-injury proliferation.

DISCUSSION

A “switching” versus “segregating” model of cortical cell ontogeny

The lineage relationship of neurons, astrocytes and oligodendrocytes in the mammalian cerebral cortex remains uncertain, and two alternative hypotheses have been proposed (Fig. 10). The first hypothesis, a “switching” model, proposes a single progenitor pool that sequentially generate neurons and glial cells at different times of development. In contrast, the “segregating” model envisions early separation of neuron- and macroglia-restricted lineages in the cerebral cortex. This model is supported by co-existence of neuronal and glial precursors in the early fetal monkey cortex (Levitt et al., 1981) and segregation of astrocyte and oligodendrocyte lineages in the embryonic rat cerebrum (LeVine and Goldman, 1988).

Previous experimental data on neuron and macroglia ontogeny were mostly generated by the retroviral lineage-tracing method. Overall, these studies suggested early divergence of neuron-, astrocyte-, and oligodendrocyte-restricted lineages in the embryonic rodent cerebrum (Grove et al., 1993; Luskin et al., 1993; Parnavelas, 1999). In recent years, this issue was revisited with genetic fate-mapping methods, including the brain lipid binding protein (BLBP) promoter- or human GFAP promoter- mediated Cre drivers, which are supposed to specifically label RG progenitors (Malatesta et al, 2003; Anthony et al., 2004). These studies concluded that RG are the common progenitors of neurons, astrocytes, and oligodendrocytes. However, because the BLBP-Cre-mediated reporter gene expression was detected as early as E10.5 (see Fig. 3B in Anthony et al., 2004), before the appearance of

GLAST+ RG in the forebrain, and since the murine RG do not express GFAP, the proposed lineage potential of RG based on BLBP-Cre mice and hGFAP-promoter should be appraised with caution.

In the present study, we used tamoxifen-inducible Nestin-CreER mice crossed to an EGFP-Cre-reporter line to re-assess the lineage origins of cortical macroglia. We show that Nestin-CreER mice not only label RG progenitors, but also mark perinatal SVZ glioblasts if tamoxifen was administered during late embryogenesis (E16-E18). Although the nestin second intron enhancer (NIE) in Nestin-CreER mice may or may not match the endogenous nestin gene expression at all developmental stages, this approach allows us to compare the lineage potential of RG (labeled by tamoxifen induction in early corticogenesis) and non-RG, perinatal SVZ glioblasts (labeled by tamoxifen-induction in late corticogenesis) in the same system. The results of our experiments bear implications on three important issues: (1) multiple origins of cortical astrocytes, (2) exclusive SVZ-glioblast origin of cortical oligodendrocytes, and (3) distinct proliferation potential between astrocytes and NG2+ OPCs after brain injury.

Multiple origins of cortical astrocytes

Accumulating evidence indicates that RG and the perinatal SVZ glioblasts both derive cortical astrocytes (Goldman, 2001). Past histological studies suggested that RG undergo a succession of morphological transformations into astrocytes in the perinatal brain (Schmechel and Rakic, 1979; Voigt, 1989; Takahashi et al., 1990). The transforming property of RG was also indicated by tissue culture experiments (Culican et al., 1990). However, these studies have never shown mitosis by RG in “astrocytic transformation”. If RG only undergo non-proliferative metamorphosis, it has to be another source of glial progenitors to account for the sudden increase of astrocytes in perinatal brains. Indeed, by injecting replication-defected retrovirus into the perinatal SVZ, Dr. Goldman and his colleagues identified a population of perinatal SVZ glioblasts, capable of active cell-proliferation and directional migration into the cortex (Levison and Goldman, 1993; Kakita and Goldman, 1999). However, the relative contributions by RG and perinatal SVZ glioblasts to cortical astrocytes are yet to be compared, and it remains uncertain whether the latter are derived from RG to serve as immediate glial progenitors.

In the present study, based on live-imaging and histological criteria (Fig. 3, 4), we showed that NIE-driven Nestin-CreER mice can mark the perinatal SVZ glioblasts by tamoxifen-induction in late-embryogenesis (E16-E18). Further, we showed that E18 tamoxifen-induction fate-mapped more simple glioblasts than RG and transitional forms combined in the newborn cerebral cortex (Table 2). Moreover, the number of labeled SVZ glioblasts increased from birth to P4 and declined afterwards, coinciding with the peak of perinatal astrocyte production (Table 2 and Fig. 7). Finally, we showed that simple glioblasts can transform into a bipolar shape in brain slice, cautioning that not all “transitional RG forms” in static histological analysis are derived from RG (Fig. 5B). Together, these results suggest the perinatal SVZ glioblasts are an essential source of cortical astrocytes, and likely have a more important contribution than RG (Fig. 10B).

Perinatal SVZ glioblasts are the principle source of cortical oligodendrocytes

Previous studies indicated three competing waves of oligodendrocyte production in the forebrain, with the third wave arising from the cerebral cortex to assume an eventually predominant role (Kessaris et al., 2006; Kessaris et al, 2008). Given this wave's temporal overlap with perinatal RG transformation, the majority of cortical oligodendrocytes may be descendants of RG.

However, here we showed that fate-mapping the progeny of RG progenitors with E10-tamoxifen induction labels astrocytes, but not oligodendrocytes in postnatal cerebral cortex (Fig. 2G; Table 1). In contrast, fate-mapping perinatal SVZ glioblasts with E18-induction labels many grey-matter and white-matter oligodendrocytes in the postnatal brain (Fig. 2I). Although we could not rule out the possibility that RG may generate the prenatal waves of oligodendrocytes that eventually undergo cell death, our results indicate that perinatal SVZ glioblasts are the primary source of oligodendrocytes that survive in the adult brain.

The lack of detection of postnatal oligodendrocytes by E10 tamoxifen-induction in Nestin-CreER mice also suggests the perinatal SVZ glioblasts are not directly derived from RG. This is because if RG give rise to perinatal SVZ glioblasts, labeling RG with E10 tamoxifen-induction should detect oligodendrocytes in postnatal brains just like labeling the SVZ glioblasts with E18-induction, but this is contrary to our observation. Instead, the fact that E18-induction, but not E10-dosing, labels cortical oligodendrocytes suggests that perinatal SVZ glioblasts mainly descend from a separate pool of NIE-negative precursors at E10 (Fig. 10B). Hence, our results support the notion of early divergence of astrocyte and oligodendrocyte lineages in the developing cerebrum, as previously proposed (LeVine and Goldman, 1988).

NG2+ OPCs are the principle proliferating cells in adult or post-injury brains

In the present study, we also examined the proliferation capacity of cortical astrocytes and oligodendrocytes beyond the neonatal period. With the combination of genetic fate-mapping and BrdU immunocytochemistry, we demonstrated cortical astrocytes quickly exhaust their proliferation capacity in the postnatal brain (< P10), whereas NG2+ OPCs possess a longer period of proliferation (approximately 10% at P30) (Fig. 7). Using this approach, we also examined the proliferation potential of cortical astrocytes and oligodendrocytes following a stab wound to the postnatal (P45) brain. These experiments reveal that, at least in the needle-stick injury model, astrocytes only respond with increased GFAP expression without resuming cell-division, while OPCs show a trend towards increased proliferation.

Our results contradict the conclusion by a recent report that astrocytes start to proliferate after stab wound injury in postnatal brains (Buffo et al., 2008). Instead, our results are more compatible with the notion that NG2+ OPCs undergo mitosis to form a reactive glial population in injured brains (Levine et al., 2001; Alonso, 2005; Baracskay et al., 2007). However, the possibility remains that more severe forms of brain injury may induce quiescent astrocytes to proliferate, presumably through re-activation of the Olig2 transcription factor expression (Chen et al., 2008).

In conclusion, by fate-mapping Nestin-CreER mice at different times, we show that RG and perinatal SVZ glioblasts are separate sources of cortical gliogenesis. Together, these results caution that a "switching" model whereby common precursors give rise to neurons, astrocytes, and oligodendrocytes as often suggested by *in-vitro* neural stem cell cultures, may not be applicable *in vivo*. Instead, our results support a scenario of early commitment and divergence of multiple lineage-restricted progenitors during embryogenesis.

Supplementary Material

Refer to Web version on PubMed Central for supplementary material.

ACKNOWLEDGMENTS

We thank Matt Kofron for assistance with conversion of confocal images to movies. This work was supported by the US National Institutes of Health grants (NS38296, NS56435 to C-Y.K.), a pilot project grant from the Barrett Cancer Center at the University of Cincinnati (to C.-Y. K.), and a CCHMC Trustee Award (to S.C. D). K.A.B. was supported by a NIH training grant (T32 ES009051).

REFERENCES

Alonso G. NG2 proteoglycan-expressing cells of the adult rat brain: possible involvement in the formation of glial scar astrocytes following stab wound. Glia. 2005; 49:318–338. [PubMed: 15494983]

Anthony TE, Klein C, Fishell G, Heintz N. Radial glia serve as neuronal progenitors in all regions of the central nervous system. Neuron. 2004; 41:881–890. [PubMed: 15046721]

Baracskay KL, Kidd GJ, Miller RH, Trapp BD. NG2-positive cells generate A2B5 positive oligodendrocyte precursor cells. Glia. 2007; 55:1001–1010. [PubMed: 17503442]

Buffo A, Rite I, Tripathi P, Lepier A, Colak D, Horn AP, Mori T, Gotz M. Origin and progeny of reactive gliosis: A source of multipotent cells in the injured brain. Proc Natl Acad Sci U S A. 2008; 105:3581–3586. [PubMed: 18299565]

Burns KA, Ayoub AE, Breunig JJ, Adhami F, Weng WL, Colbert MC, Rakic P, Kuan CY. Nestin-CreER mice reveal DNA synthesis by nonapoptotic neurons following cerebral ischemia hypoxia. Cereb Cortex. 2007; 17:2585–2592. [PubMed: 17259645]

Cai J, Chen Y, Cai WH, Hurlock EC, Wu H, Kernie SG, Parada LF, Lu QR. A crucial role for Olig2 in white matter astrocyte development. Development. 2007; 134:1887–1899. [PubMed: 17428828]

Chen Y, Miles DK, Hoang TN, Shi J, Hurlock E, Kernie SG, Lu QR. The basic helic-loop-helic transcription factor Olig2 is critical for reactive astrocyte proliferation after cortical injury. J Neurosci. 2008; 28:10983–10989. [PubMed: 18945906]

Culican SM, Baumrind NL, Yamamoto M, Pearlman AL. Cortical radial glia: identification in tissue culture and evidence for their transformation to astrocytes. J Neurosci. 1990; 10:684–692. [PubMed: 2303868]

Dawson MR, Polito A, Levine JM, Reynolds R. NG2-expressing glial progenitor cells: an abundant and widespread population of cycling cells in the adult rat CNS. Mol Cell Neurosci. 2003; 24:476–488. [PubMed: 14572468]

Fujita S. An autoradiographic study on the origin and fate of the sub-pial glioblast in the embryonic chick spinal cord. J. Comp. Neurology. 1965; 124:51–9.

Gal JS, Morozov YM, Ayoub AE, Chatterjee M, Rakic P, Haydar TF. Molecular and morphological heterogeneity of neural precursors in the mouse neocortical proliferative zones. J Neurosci. 2006; 26:1045–1056. [PubMed: 16421324]

Goldman, JE. Developmental origins of astrocytes. In: Jessen, KR.; Richardson, WD., editors. Glial cell development. Oxford UP; New York: 2001. p. 55-74.

Grove EA, Williams BP, Li DQ, Hajihosseini M, Friedrich A, Price J. Multiple restricted lineages in the embryonic rat cerebral cortex. Development. 1993; 117:553–561. [PubMed: 8330526]

Hirano M, Goldman JE. Gliogenesis in rat spinal cord: evidence for origin of astrocytes and oligodendrocytes from radial precursors. J Neurosci Res. 1988; 21:155–167. [PubMed: 3216418]

Hunter KE, Hatten ME. Radial glial cell transformation to astrocytes is bidirectional: regulation by a diffusible factor in embryonic forebrain. Proc Natl Acad Sci U S A. 1995; 92:2061–2065. [PubMed: 7892225]

Kakita A, Goldman JE. Patterns and dynamics of SVZ cell migration in the postnatal forebrain: monitoring living progenitors in slice preparations. Neuron. 1999; 23:461–472. [PubMed: 10433259]

Kessaris N, Fogarty M, Iannarelli P, Grist M, Wegner M, Richardson WD. Competing waves of oligodendrocytes in the forebrain and postnatal elimination of an embryonic lineage. Nat Neurosci. 2006; 9:173–179. [PubMed: 16388308]

Kessaris N, Pringle N, Richardson WD. Specification of CNS glia from neural stem cells in the embryonic neuroepithelium. Philos Trans R Soc Lond B Biol Sci. 2008; 363:71–85. [PubMed: 17282992]

Levine JM, Reynolds R, Fawcett JW. The oligodendrocyte precursor cell in health and disease. Trends Neurosci. 2001; 24:39–47. [PubMed: 11163886]

LeVine SM, Goldman JE. Embryonic divergence of oligodendrocyte and astrocyte lineages in developing rat cerebrum. J Neurosci. 1988; 8:3992–4006. [PubMed: 3054008]

Levison SW, Goldman JE. Both oligodendrocytes and astrocytes develop from progenitors in the subventricular zone of postnatal rat forebrain. Neuron. 1993; 10:201–212. [PubMed: 8439409]

Levitt P, Cooper ML, Rakic P. Coexistence of neuronal and glial precursor cells in the cerebral ventricular zone of the fetal monkey: an ultrastructural immunoperoxidase analysis. J Neurosci. 1981; 1:27–39. [PubMed: 7050307]

Luskin MB, Parnavelas JG, Barfield JA. Neurons, astrocytes, and oligodendrocytes of the rat cerebral cortex originate from separate progenitor cells: an ultrastructural analysis of clonally related cells. J Neurosci. 1993; 13:1730–1750. [PubMed: 8463848]

Malatesta P, Hartfuss E, Gotz M. Isolation of radial glial cells by fluorescent-activated cell sorting reveals a neuronal lineage. Development. 2000; 127:5253–5263. [PubMed: 11076748]

Malatesta P, Hack MA, Hartfuss E, Kettenmann H, Klinkert W, Kirchhoff F, Gotz M. Neuronal or glial progeny: regional differences in radial glia fate. Neuron. 2003; 37:751–764. [PubMed: 12628166]

Marshall CA, Novitch BG, Goldman JE. Olig2 directs astrocyte and oligodendrocyte formation in postnatal subventricular zone cells. J Neurosci. 2005; 25:7289–7298. [PubMed: 16093378]

Mori T, Tanaka K, Buffo A, Wurst W, Kuhn R, Gotz M. Inducible gene deletion in astroglia and radial glia--a valuable tool for functional and lineage analysis. Glia. 2006; 54:21–34. [PubMed: 16652340]

Noctor SC, Flint AC, Weissman TA, Dammerman RS, Kriegstein AR. Neurons derived from radial glial cells establish radial units in neocortex. Nature. 2001; 409:714–720. [PubMed: 11217860]

Parnavelas JG. Glial cell lineages in the rat cerebral cortex. Exp Neurol. 1999; 156:418–429. [PubMed: 10328946]

Rakic P. Elusive radial glial cells: historical and evolutionary perspective. Glia. 2003; 43:19–32. [PubMed: 12761862]

Sauvageot CM, Stiles CD. Molecular mechanisms controlling cortical gliogenesis. Curr Opin Neurobiol. 2002; 12:244–249. [PubMed: 12049929]

Schmechel DE, Rakic P. A Golgi study of radial glial cells in developing monkey telencephalon: morphogenesis and transformation into astrocytes. Anat Embryol (Berl). 1979; 156:115–152. [PubMed: 111580]

Takahashi T, Misson JP, Caviness VS Jr. Glial process elongation and branching in the developing murine neocortex: a qualitative and quantitative immunohistochemical analysis. J Comp Neurol. 1990; 302:15–28. [PubMed: 2086612]

Voigt T. Development of glial cells in the cerebral wall of ferrets: direct tracing of their transformation from radial glia into astrocytes. J Comp Neurol. 1989; 289:74–88. [PubMed: 2808761]

Watanabe M, Sakurai Y, Ichinose T, Aikawa Y, Kotani M, Itoh K. Monoclonal antibody Rip specifically recognizes 2',3'-cyclic nucleotide 3'-phosphodiesterase in oligodendrocytes. J Neurosci Res. 2006; 84:525–533. [PubMed: 16786579]

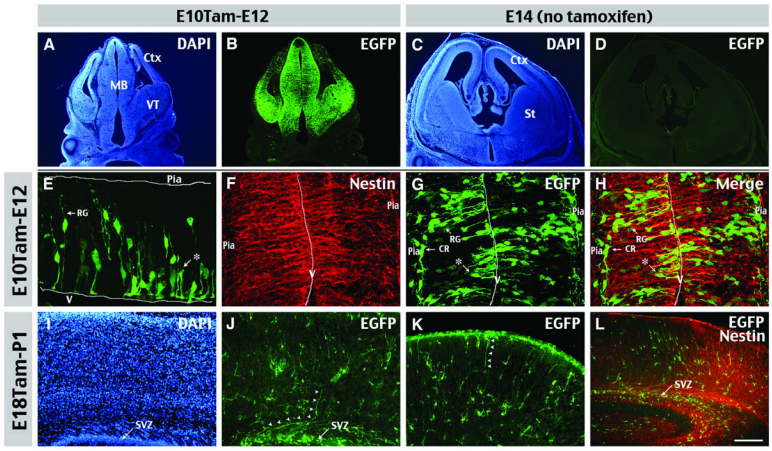

Figure 1. Nestin-CreER mice lineage-trace radial glia and SVZ glioblasts

The identities of labeling progenitors were examined in Nestin-CreER/EGFP-Cre-Reporter (Bitransgenic) embryos at 2 days following tamoxifen (Tam)-induction at E10.5 (A-B, E-H) or E18.5 (I-L). ***A, B,*** E10Tam-E12 chase labeled many EGFP+ cells in the midbrain (MB) and the ventral telencephalon (VT), and a few cells in the developing cerebral cortex (Ctx). ***C, D W***ithout Tam-induction, there were no EGFP+ cells in E14 bi-transgenic embryos. ***E,*** E10Tam-E12 chase labeled many EGFP+ cell profiles, including radial glia (RG) and short neural precursors (asterisk). V: ventricular surface. ***F, G, H,*** Double-labeling of E10Tam-E12 cortex shows RG and short neural precursors express nestin, whereas Cajal-Retzius cells (CR) near the pia do not. ***I-L,*** E18Tam-P1 chase labeled many EGFP+ cells in the subventricular zone (SVZ) and a few cells with curved radial fibers (arrowheads) which are labeled by nestin (L) Scale bar: 400μm in A, B; 50μm in C, D; 50μm in E-H; 100μm in I-K; 200μm in L.

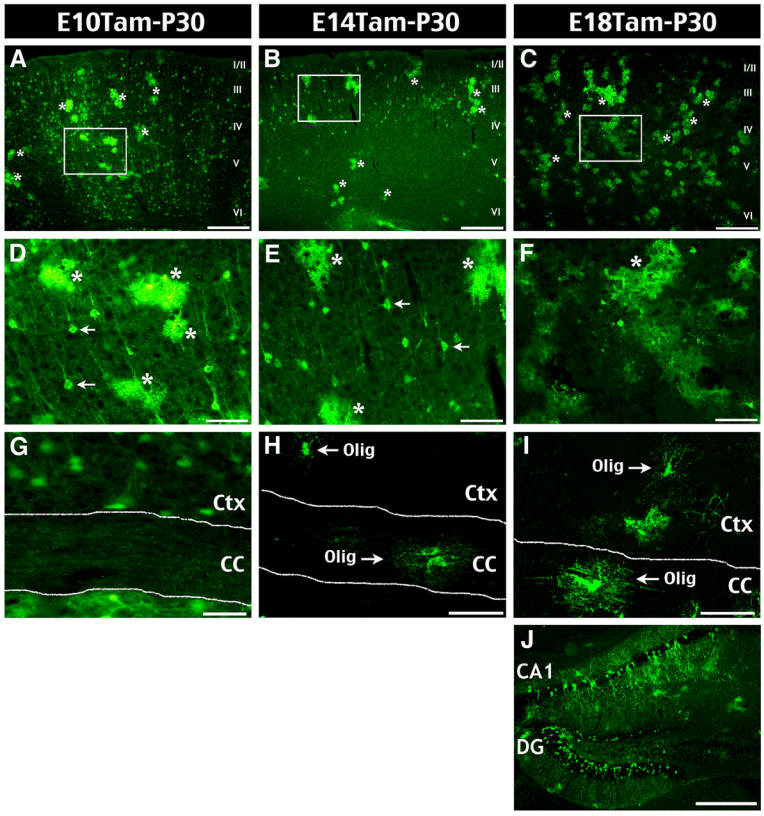

Figure 2. Genetic fate-mapping shows early divergent oligodendrocyte precursors

We examined EGFP+ cells in the cerebral cortex of P30 bitransgenic mice that were dosed with Tam on E10.5, E14.5, or E18.5. ***A, D, G,*** E10 Tam-induction labeled EGFP+ astrocytes (asterisk) and neurons in all layers of the cerebral cortex (A, D), but no oligodendrocytes in the cortex (Ctx) or the corpus callosum (CC) (G). ***B, E, H,*** E14-induction labeled astrocytes and neurons of upper cortical layers, as well as a few oligodendrocytes (Olig) in both Ctx and CC (H). ***C, F, I, J,*** E18-induction labeled astrocytes and oligodendrocytes, but no cortical neurons (C-I); however, perinatal-born hippocampal neurons were labeled by induction at E10, E14, and E18 (J). Scale bars: 300mm in A-C, J; 50mm in D-I.

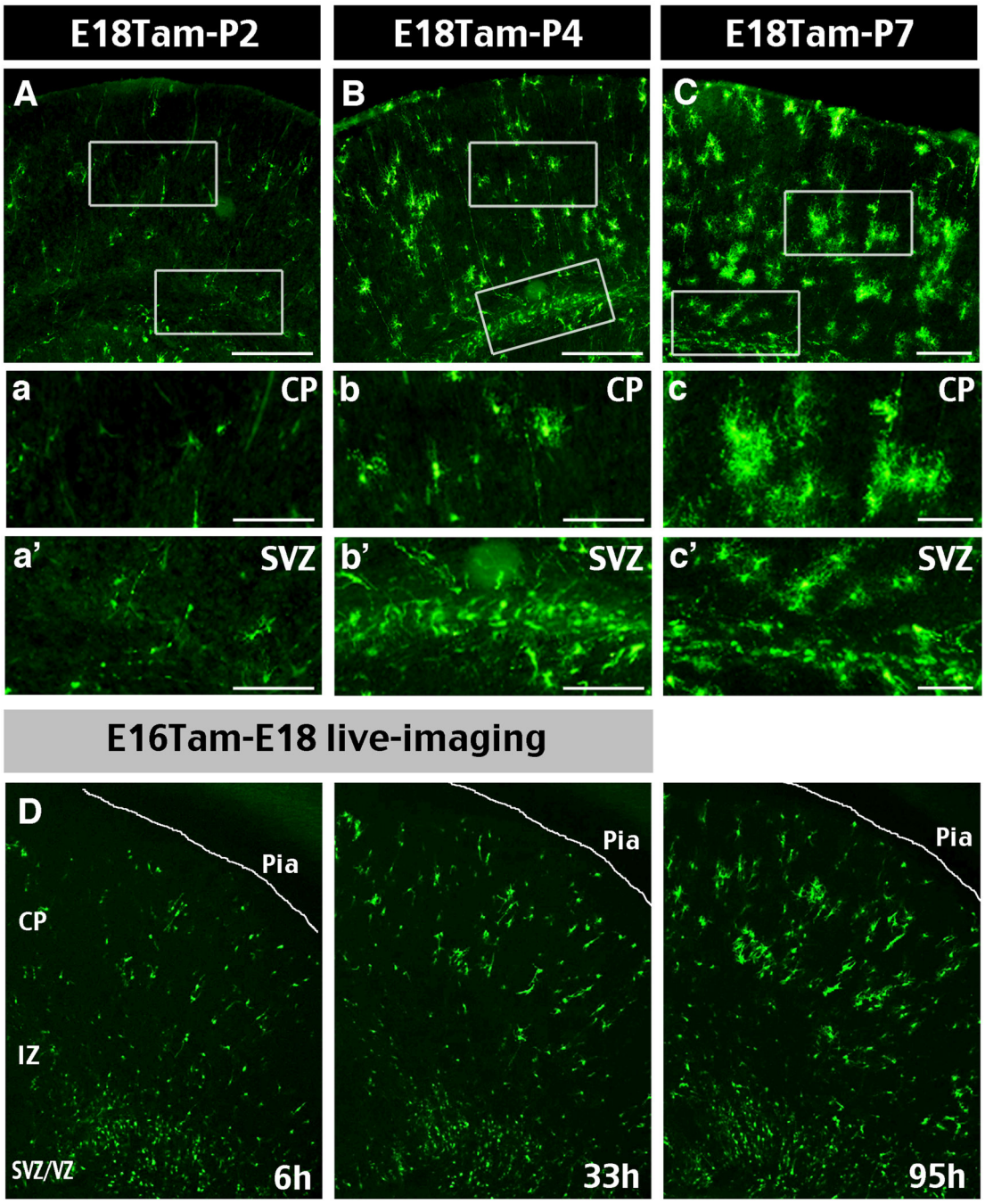

Figure 3. Late embryonic induction in Nestin-CreER mice labels perinatal SVZ glioblasts

A-C, Cortical gliogenesis was examined using Nestin-CreER/EGFP-Cre-Reporter mice dosed with Tam on E18 and sacrificed at P2, P4, or P7. ***a-c,*** Magnified images of boxed areas in A-C showed astrocytes in the cortical plate (CP) displayed increasingly branched cytoplasmic processes from P2 to P7. ***a′-c′,*** There was an increase of EGFP+ glioblasts in the subventricular zone (SVZ) from P2 to P4, then declined from P4 to P7. ***D,*** Time-lapse video microscope was used to image the proliferation and maturation of glial progenitors over 4 days following the E16Tam-E18 chase protocol (also see Supplementary Movie 1).

CP: cortical plate, IZ: intermediate zone; SVZ/VZ: subventricular and ventricular zones. Scale bars: 300μm in A-C; 120μm in a-c and a′-c′.

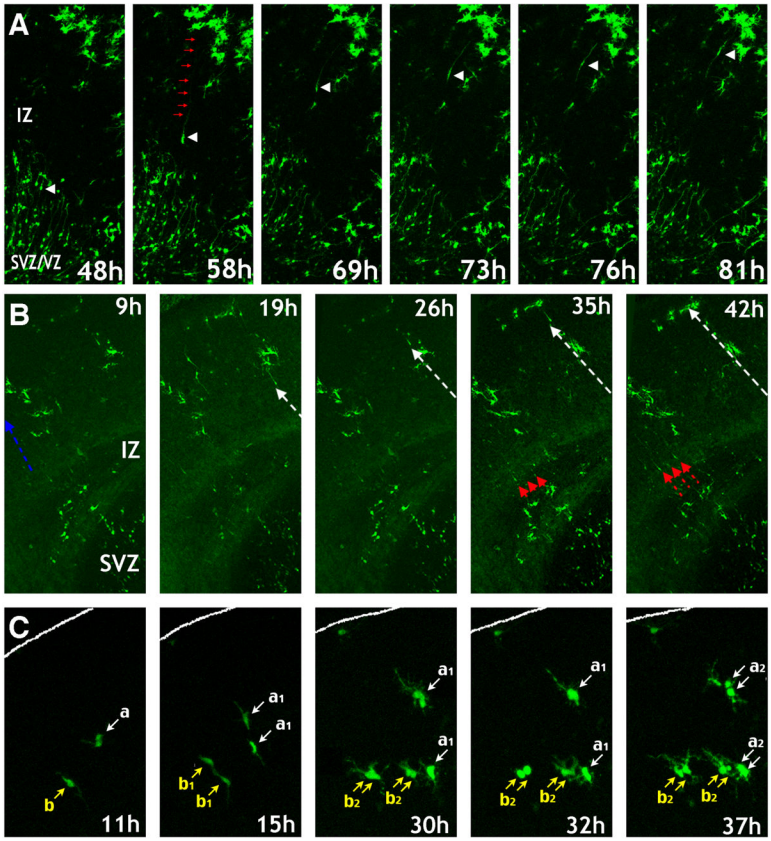

Figure 4. Live-imaging of SVZ glioblasts migration and proliferation in brain slices

Time-lapse video microscopy was used to image the migration and proliferation of glial progenitors in slices of E18 forebrain following E16 Tam-induction. ***A,*** Global view of glioblast proliferation and maturation over 4 days (see also supplementary movie 1). ***A,*** Translocation mode of glioblast migration from the SVZ/VZ across the intermediate zone (IZ) (Supplementary Movie 2). ***B,*** Locomotion mode of glioblasts migration in continuous waves (white and red arrows) from the SVZ towards the pial surface (Supplementary Movie 3). ***C,*** Simple glioblasts may undergo several rounds of division in the cortex (pial surface outlined) (Supplementary Movie 4). All times indicate hours in culture.

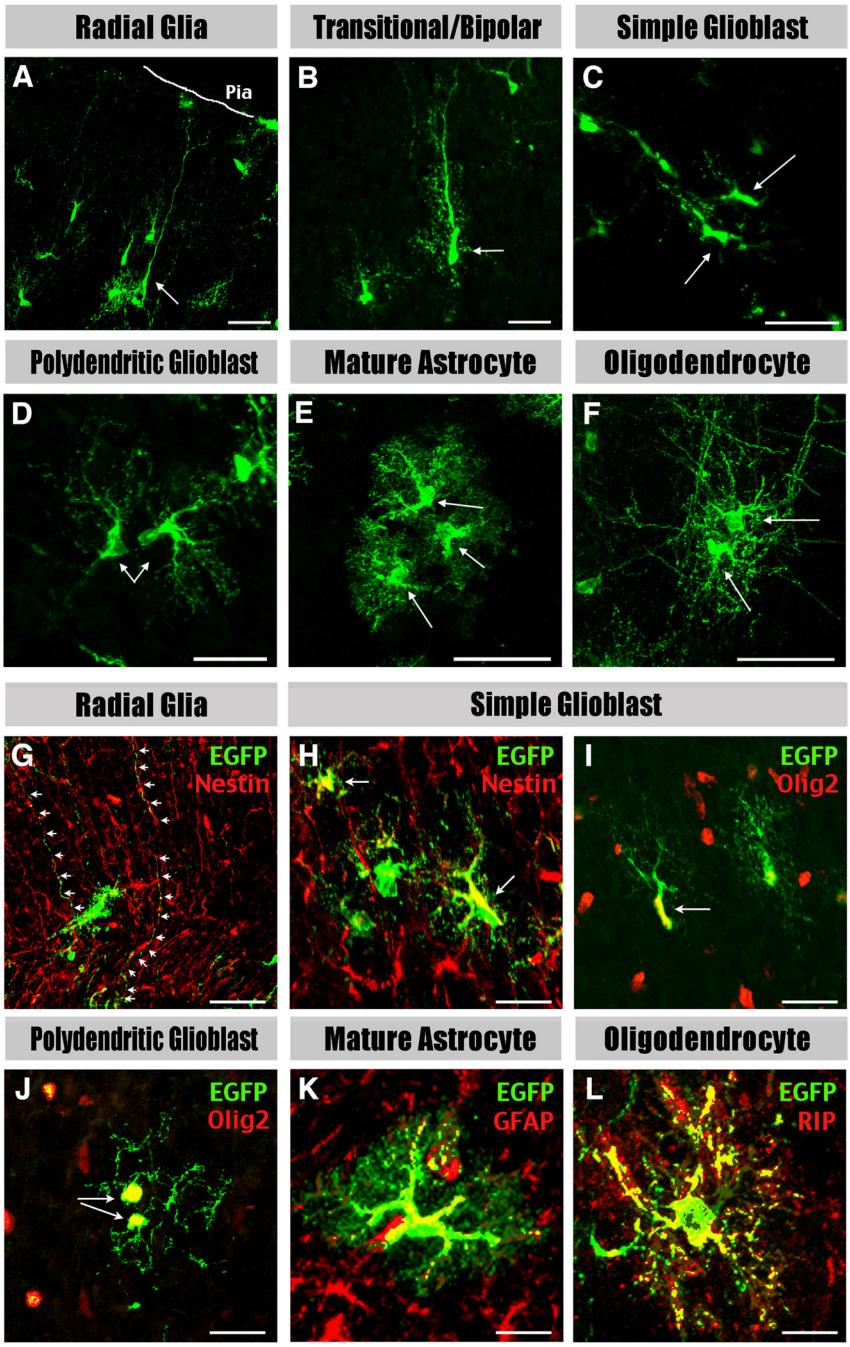

Figure 5. Classification of the descendants of RG and SVZ glioblast progenitors

Cortical glial cell types characterized at different postnatal stages include: ***A,*** Radial glia have characteristic radial processes. ***B,*** Transitional/bipolar cells have transitional morphologies shorter and thicker radial processes. ***C,*** Simple glioblasts have short leading processes. ***D,*** Polydendritic glioblasts have the basic architecture but lack the fine branching of mature astrocytes. ***E,*** Mature astrocytes have multiple processes with extensive branching. ***F,*** Oligodendrocytes have fine lacy processes aligned in spherical or parallel sheets. ***G-L,*** Radial glia express Nestin in their processes (arrows in G), simple glioblasts

express Nestin (H) and Olig2 (I), polydendritic glioblasts express Olig2 (J), mature astrocytes express GFAP (K), and oligodendrocyte express RIP (L). Shown in G-L are the merged images. For single-channel images see Supplemental Figure 1. Scale bar: 50μm in A-F; 20μm in G-L.

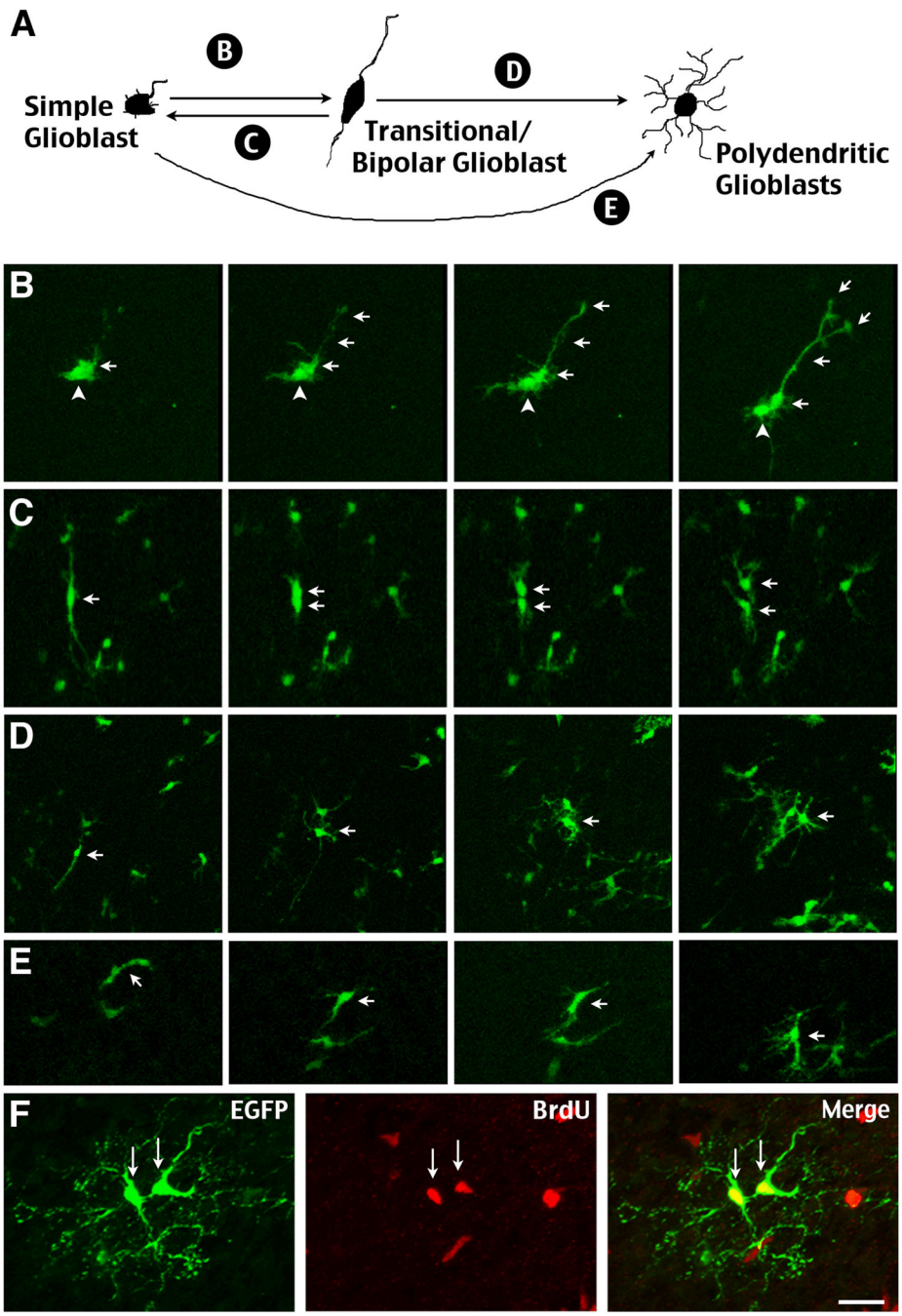

Figure 6. Simple glioblasts and transitional RG show reciprocal metamorphosis

A, Summary of morphological transformations between various forms of glioblasts in the perinatal cortex revealed by time-lapse microscopy. (see also supplementary movie 5). ***B,*** Simple glioblasts may extend processes similar to bipolar forms. ***C,*** Bipolar transitional forms can become simple or polydendritic glioblasts following mitosis. ***D,*** Transitional forms retract radially aligned processes and undergo branching to become mature glia. ***E,*** Simple glioblasts also undergo branching to become mature glia. **F,** The proliferation of

polydendritic glioblasts is marked *in vivo* by incorporation of BrdU administered 30 minutes prior to sacrifice. Scale bars: 20μm in F.

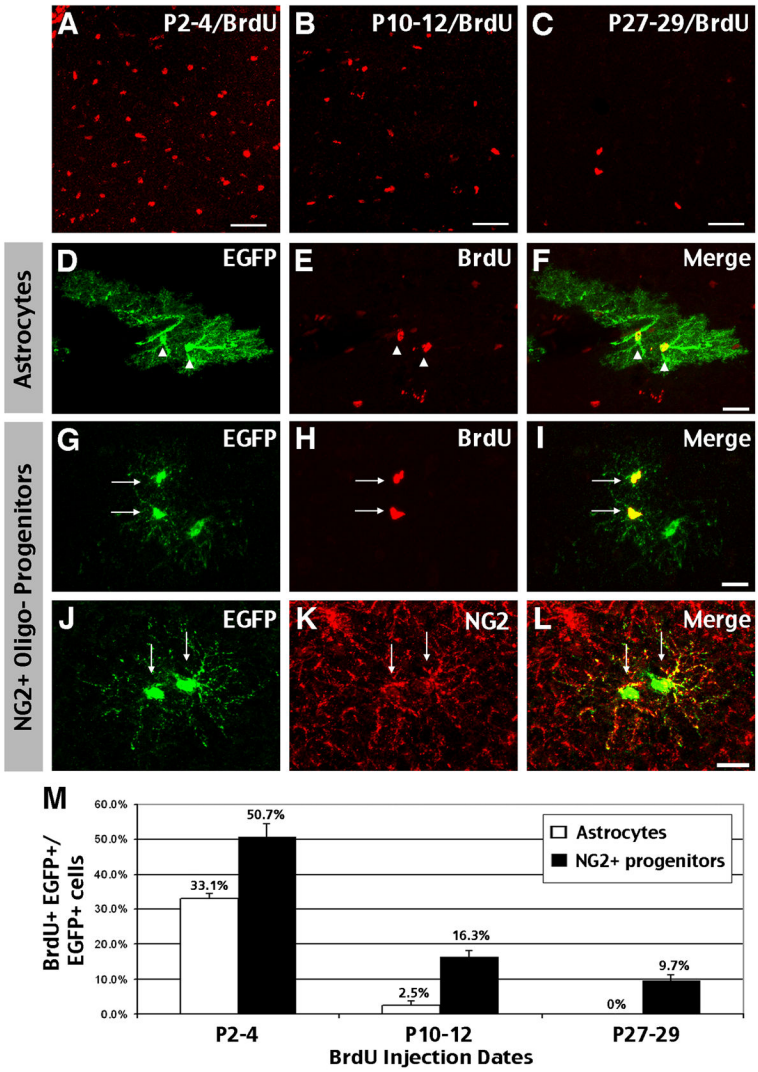

Figure 7. Oligodendrocytes have a longer time-frame of proliferation than astrocytes in the postnatal cerebral cortex

A-C, M, Administration of BrdU over a three-day dosing period (P2-4, P10-12, and P27-29) showed marked reduction of proliferation in the cortex in the first postnatal month. ***D-F,*** Astrocytes pre-labeled by E18 tamoxifen-dosing were readily labeled by P2-P4 BrdU injection, but their proliferation is curtailed by P10 (M). ***G-I***, Oligodendrocyte precursors labeled by BrdU often appear as doublets. J-L, oligodendrocyte precursors predominantly express NG2. ***M***, Quantification of BrdU+ cells among EGFP+ astrocytes and NG2+ precursors in the first postnatal month. Astrocytes showed a rapid decline of proliferative capacity, while 9.7% oligodendrocytes still incorporated BrdU at P27-29. Scale bars: 50μm A-C, 20μm D-L.

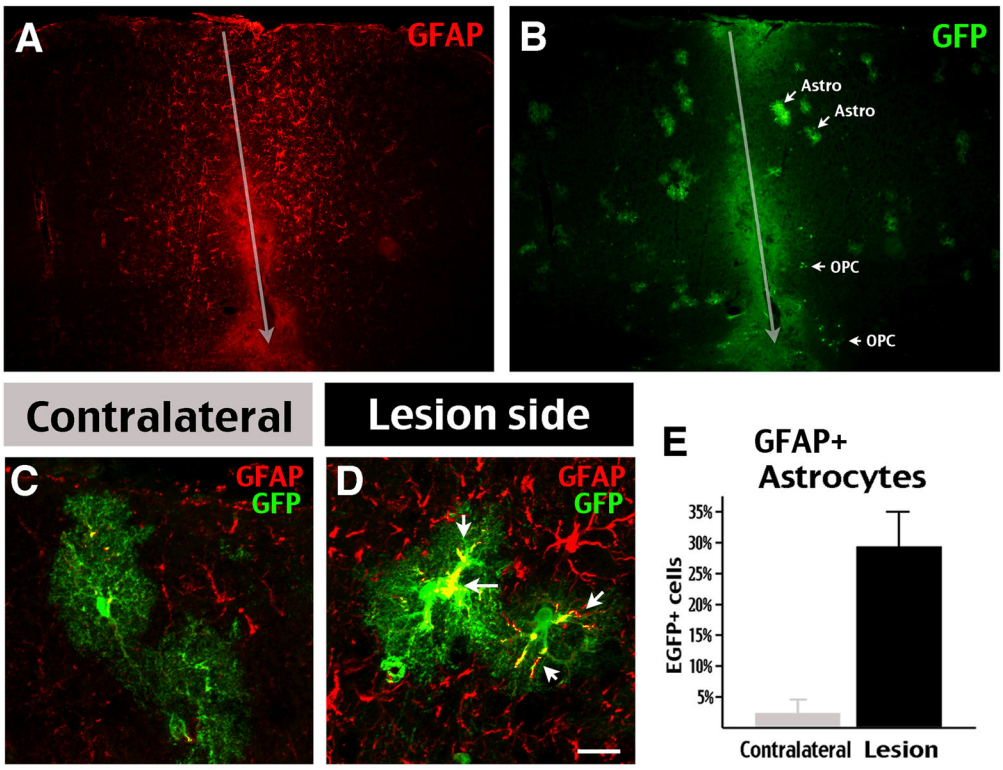

Figure 8. Stab-wound injury induces GFAP expression by astrocytes in adult brains

Bi-transgenic mice dosed with Tam at E18 were challenged by a needlestick wound at P45, and sacrificed on P49. ***A, B,*** The stab-wound robustly upregulated GFAPnear the needle insertion track (arrow). ***C, D,*** Following the unilateral needlestick stab-wound, EGFP+ astrocytes on the lesion side express a higher amount of GFAP in the proximal and distal branches (D), than on the contralateral side (C). ***E,*** The percentage of GFAP/EGFP double-labeled cells among all fate-mapped astrocytes was increased within the 1mm radius of the needlestick track in the cerebral cortex compared to the contralateral side (n=4). Scale bar: 200μm in A, B; 50μm in C, D.

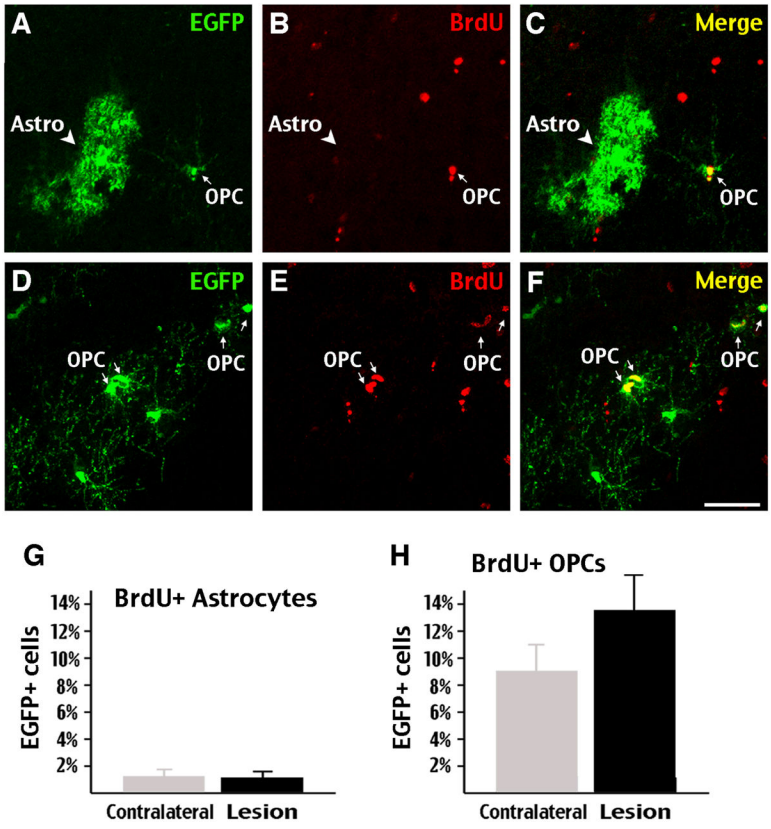

Figure 9. Oligodendrocyte progenitors, but not GFAP-astrocytes, respond to the stab-wound injury with proliferation

In the stab-wound experiment described in Figure 8, BrdU was injected daily from P42 to P48. BrdU/EGFP double-labeling showed the vast majority of EGFP+ astrocytes (arrowhead in A-C) did not incorporate BrdU after the stab-wound injury. In contrast, many EGFP+ oligodendrocyte precursors (arrows in D-I) incorporated BrdU after the stab-wound injury. ***G,*** The percentage of BrdU-incorporated astrocytes remained unchanged on the lesion side of the brain after stab-wound injury. ***H,*** However, the percentage of BrdU+/EGFP+ oligodendrocyte precursors (OPCs) trended upward on the lesion side (n=4) (p=0.16 by two-tailed student's *t*-test). Scale bars: 50μm

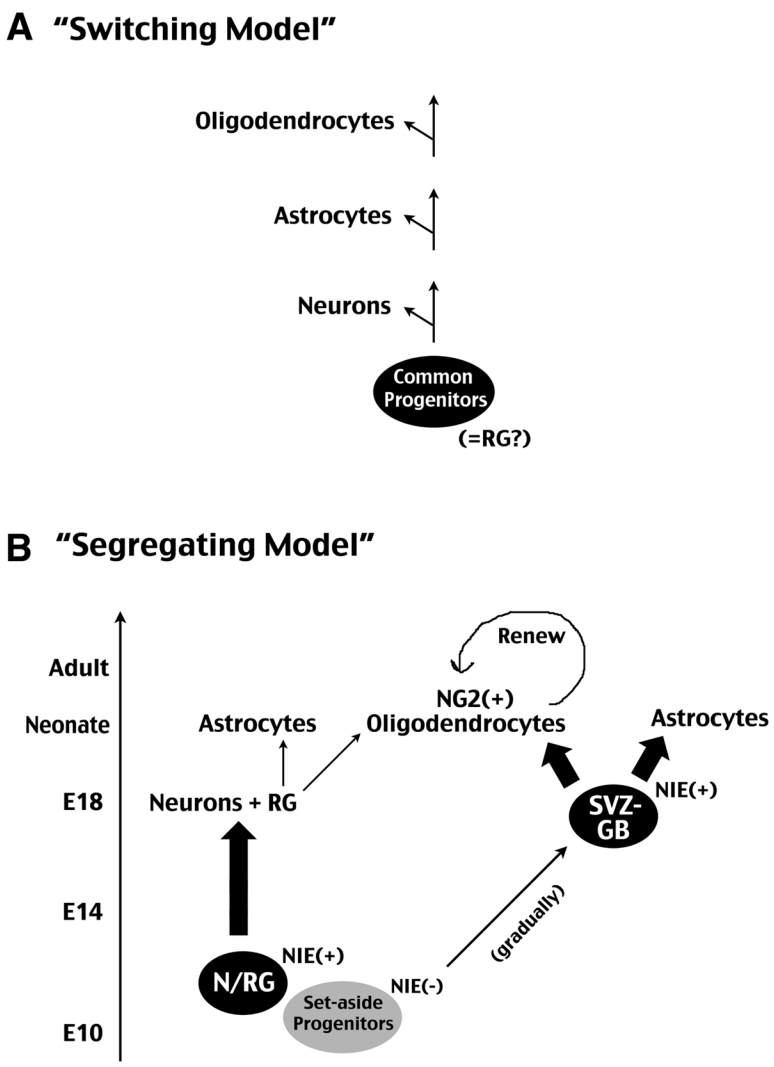

Figure 10. Two prototypic models to explain the lineage relationship among major cortical cell types

A, The "switching" model proposes a common progenitor pool that sequentially gives rise to neurons, astrocytes, and oligodendrocytes. This common progenitor population may be radial glia (RG). ***B,*** The "segregating" model proposes early divergence of neuron and macroglial lineages in the developing cerebral cortex. We suggest that a set of precursors expressing Nestin second-intron enhancer (NIE) around E10 is the principle neuronal progenitor (N) that may overlap with the RG lineage. The precursors of the subventricular zone glioblasts (SVZ-GB) are NIE-negative at E10 and gradually upregulate NIE in later development. The SVZ-GB progenitor pool eventually give rise to the bulk of postnatal astrocytes and NG2+ oligodendrocytes. In postnatal brains, NG2+ oligodendrocyte precursors maintain a renewal capacity and respond to injury.

Table 1

	Timing of tamoxifen induction		
	E10	**E14**	**E18**
Cortical Neurons	All layers	Upper layers	-
Hippocampal Neurons	+	+	+
Cortical Astrocytes	+	+	+
GM/WM Oligodendrocytes	-	+	+

Table 2

Quantification of glioblasts and glial cells, fate-mapped by E18 tamoxifen-induction, in the cerebral cortex between P2 and P10.

Cell Type	P2 (n=121)	P4 (n=572)	P7 (n=433)	P10 (n=375)
Radial Glia	21.5% (n=26)	14.9% (n=85)	7.4% (n=32)	1.1% (n=4)
Transitional/Bipolar	14.0% (n=17)	10.5% (n=60)	4.4% (n=19)	0.5% (n=2)
Simple Glioblast	31.4% (n=38)	30.4% (n=174)	8.3% (n=36)	13.3% (n=50)
Polydendritic Glioblast	33.1% (n=40)	42.1% (n=241)	33.0% (n=143)	26.4% (n=99)
Mature Astrocyte	0.0% (n=0)	2.1% (n=12)	37.6% (n=163)	40.0% (n=150)
Oligodendrocyte	0.0% (n=0)	0.0% (n=0)	9.2% (n=40)	32.5% (n=122)